Development of an Electro-Optically Tuned Optical Coherence Tomography System for Imaging Dental Lesions

Vani Damodaran and Nilesh J. Vasa

Abstract— **A conventional optical coherence tomography (OCT) system was set up in-house to image early dental caries, identify gap formation in the bonding interface for restoration and secondary caries. Two-dimensional images of tooth samples was obtained and dental defect were identified. A novel electro-optic tuning system is proposed in order to improve scanning speed and to perform noiseless imaging. Preliminary studies were conducted with two crystals namely, $LiNbO_3$ (Lithium Niobate) and KTP (Potassium Titanyl Phosphate) using a SLED source for OCT system and the simulated and experimental results were found to be qualitatively similar. The tuning range for $LiNbO_3$ and KTP was found to be in the order of few micrometers whereas KTN (Potassium Tantalate Niobate) using the quadratic electro-optic effect is expected to show scanning range of tens of micrometers. KTN based hybrid scanning for dental caries imaging is also planned.**

I. Introduction

In recent years, there has been a growing interest in oral health monitoring. One of the most prevalent chronic oral diseases worldwide is dental caries. Caries are formed due to the complex interaction between the tooth surface and the biofilm overlaying it [1]. The mineral equilibrium of the tooth is affected, from early caries characterized by subsurface mineral loses to tooth substance being lost when unattended leading to cavity formation where physical intervention becomes necessary [2]. Caries identified at early stages can be arrested through preventive therapies [3]. In the case of heavy demineralisation and tooth restoration procedure, there is a need for marginal adaptation of the restoration for the treatment to be a success. Due to the morphology of the tooth surface and shrinkage of the filling, there may be gap formation at the bonding interface, which enables the onset of secondary caries, affecting the longevity of the restoration and onset of secondary caries [4]. Therefore, there is a need for early detection of caries for facilitating non-invasive reversal and detection of secondary caries formation in restorative procedure. Conventional diagnostic methods used to detect caries are visual inspection, tactile inspection and radiography [5]. These methods can detect caries only after it has progressed to deeper layers in the tooth or up to the bone. At this stage, physical removal of the infected area is required. Early caries are characterized by intact tooth surface with subsurface mineral loss and hence cannot be identified using conventional systems [6].

Advancement in optical technology has led to the development of non-invasive or non-contact optical imaging techniques. Optical imaging has several advantages of being non-ionizing, real time and high resolution, also providing functional information. Optical imaging uses the optical properties of the biological tissues such as the refractive indices of the tissue compositions and the tissue structure. One such imaging technique is an Optical Coherence Tomography (OCT). This imaging technique provides high resolution morphologic depth images of the tooth. It produces cross-sectional images of the internal microstructure in the tissue by measuring echoes of backscattered light [7]. OCT can be used to produce two and three-dimensional images of the tooth.

In conventional Time Domain Optical Coherence Tomography (TDOCT) system, depth scans are produced by measuring the intensity of back-scattered light from various layers of a sample by a scanning mechanism. Scanning inside the tooth sample is performed by moving a reference mirror in micrometer order present in the interferometric setup. This scanning mechanism is generally implemented using a mechanical stepper motor system or a piezoelectric system. The mechanical system involves backlash for forward-reverse motions, operates at low speeds and involves vibrations. Interferometric systems are very sensitive to vibrations and pick them up as noise affecting the diagnosis output. Piezoelectric system also involves mechanical movement of the reference mirror and lacks precise positioning on continuous scanning due to hysteresis.

In the current study, a novel method of scanning based on an electro-optic effect is proposed. This effect allows a high frequency phase modulation due to faster response time. The advantage of the electro-optic tuning is the absence of moving parts and high operating speeds than electro-mechanical drives. The electro-optic device involves change in refractive index of a material in a controlled manner by applying an electric field. The changes in the refractive index can translate into a number of optical parameters being modified, such as phase, polarization, or deflection, as it propagates through the device [8]. In the present study, conventional OCT system has been setup and tooth samples with early caries and restoration were imaged. A proof of concept study of the electro-optic based scanning technique for the OCT system is proposed and demonstrated.

Vani Damodaran is with the Indian Institute of Technology Madras, Chennai 600036, Tamil Nadu, India (phone: 0091-44-22574706; e-mail: vanidamodaran@gmail.com).

Nilesh J. Vasa is with the Indian Institute of Technology Madras, Chennai 600036, Tamil Nadu, India (e-mail: njvasa@iitm.ac.in)

978-1-4244-7929-0/14/$26.00 ©2014 IEEE

II. Optical Coherence Tomography

The OCT system is based on a Michelson interferometer. and the interference signal recorded using a photodetector or a camera provides imaging information. Interference occurs only when the Optical Path-length Difference (OPD) between the sample arm and reference arm is within the coherence length of the source being used. Coherence length is inversely proportional to the spectral width of the source and it represents the resolution of the system. Coherence length [9] can be estimated using (1),

$$l_c = \frac{2\ln 2}{\pi}\left(\frac{\lambda^2}{\Delta\lambda}\right) \quad (1)$$

where, l_c is the coherence length, λ is the center wavelength and $\Delta\lambda$ is the bandwidth of the source. In order to understand the working of OCT system with a broadband superluminescent light emitting diode (SLED) source, the OCT system was simulated based on the electromagnetic field propagation. A source was simulated with a center wavelength of 840 nm, spectral width of 48 nm and with a Gaussian spectral profile.

The intensity I of the interference signal was estimated for the movement of reference mirror. The interference signal is plotted as shown in Fig. 1. The coherence length can be estimated from the full-width at half maximum (FWHM) of the interference signal and was found to be 6.26 µm. The value of the coherence length based on the theoretical simulation was approximately matching with the analytical calculation of 6.33 µm given by (1).

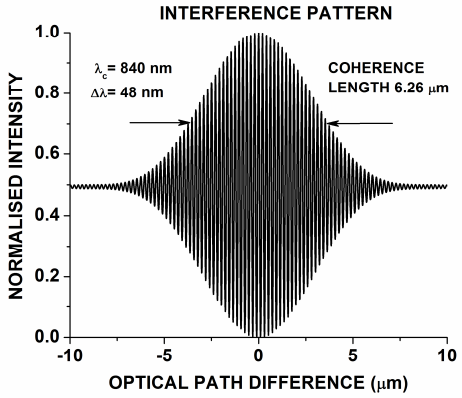

Fig. 1. Simulated OCT interference signal

III. Electro-Optic Based Scanning System

The proposed system of electro-optic based scanning is shown in Fig. 2. An electro-optic crystal is inserted in the reference arm of the interferometer. This system works on the principle of Pockels or Kerr effect [10].

A high voltage ac/dc supply is connected across the crystal as shown in Fig. 3. The applied voltage changes the refractive index of the crystal. A linear relationship exists between the applied voltage and change in refractive index and this result in phase modulation of light passing through it.

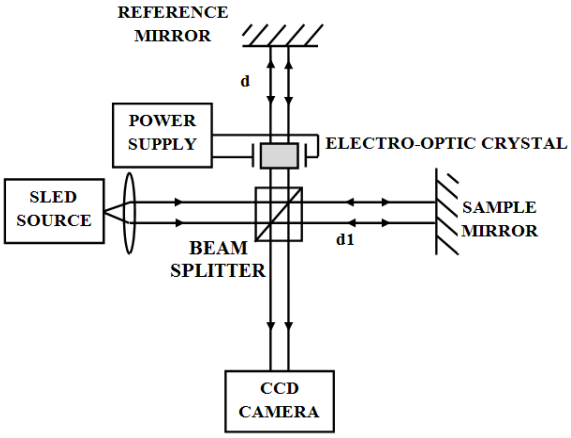

Fig. 2. Electro-optic based scanning system

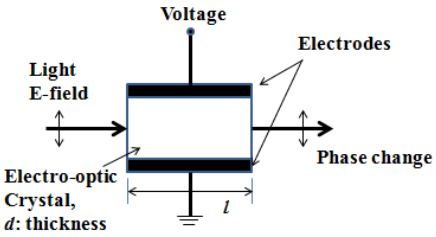

Fig. 3. Electro-optic phase modulation

Different electro-optic crystals, such as Lithium Niobate ($LiNbO_3$), Potassium Titanyl Phosphate ($KTiOPO_4$), Potassium Tantalate Niobate ($KTa_{1-x}Nb_xO_3$, KTN) etc. can be considered for such application. The change in refractive index is as shown in (2) [11].

$$\Delta n = \pm\frac{n^3}{2} \times \gamma \times E \quad (2)$$

where, Δn is the change in refractive index due to the applied electric field E ($=V/d$), n is the refractive index of the material, γ is the electro-optic coefficient. This change in refractive index induces a phase difference in the light passing through it thereby producing the same effect as that of a linear movement of the reference mirror.

As a typical case for $LiNbO_3$ crystal (9x9x25 mm), if we consider propagation of light along the optic axis (z-direction) with ordinary polarization (parallel to y-direction), the refractive index change Δnexperienced by light can be evaluated by using (2) where n is 2.278 (He-Ne) and 2.274 (Diode laser) for LiNbO3, γ_{22} is 7 pm/V. On the other hand for $KTiOPO_4$ crystal (3x3x12 mm), the resultant refractive index change Δndue to applied electric field for light propagating along the optic axis (x-direction) with extraordinary polarization (parallel to z-direction) can be evaluated, where n is 1.773 (He-Ne) and 1.771 (Diode laser), γ_{33} is 36.3 pm/V as described in (2) [12]. The effective change in the optical path length due to the change in

refractive index under the applied electric field can be described by (3),

$$L_{path} = \Delta n \times l \quad (3)$$

where, Δn is change in refractive index and l is the length of the crystal. However a high electric field is needed to obtain a useful optical phase change and the corresponding change in the optical path-length difference. In order to improve the scanning range, a crystal, such as Potassium Tantalate Niobate ($KTa_{1-x}Nb_xO_3$, KTN), which possesses a large electro-optic (γ_{11} is 2200 pm/V) can be considered. In a tetragonal phase KTN posses non-centrosymmetric phase and linear electro-optic effect can be observed. Normally, at room temperature KTN has a cubic phase and has inversion symmetry. In this phase, KTN possesses quadratic electro-optic effect (the Kerr effect) which is proportional to the square of the applied electric field. In this case, the resultant change in the refractive index is given by (4) [13],

$$\Delta n = -\frac{1}{2} n^3 s_{11} E_{11}^2 \quad (4)$$

where s_{11} is the quadratic electro-optic coefficient and E_{11} is the applied electric field.

IV. Experimental Study

A. Dental OCT

An Optical Coherence Tomography system was developed in-house with SLED source (840 nm, spectral width 48 nm, Exalos). The reference mirror was moved in steps of 0.125 µm using a micrometer stage (MTS6565-1, resolution 0.125 µm, Holmarc Opto-Mechatronics). The interference pattern was recorded using a CCD camera (acA1600-20gm, Basler) and the data acquisition system (NI PXIe-1071).

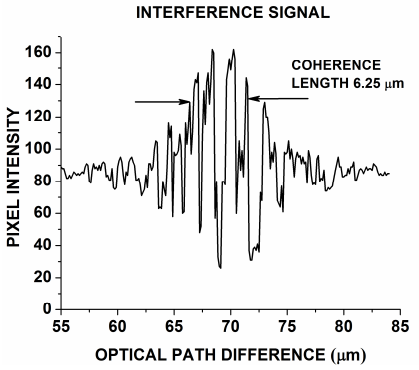

Fig. 4. Experimental TDOCT interference signal

Images were recorded for each step and the maximum intensity was analysed in order to plot the envelope of the interference pattern as shown in Fig. 4. The resolution was found to be 6.25 µm. This nearly matches with the simulated and analytical values of coherence length.

An extracted tooth sample was scanned axially in steps of 3 µm and laterally in steps of 25 µm using a micrometer stage (MTS6565-1, resolution 0.125 µm, Holmarc Opto-Mechatronics). The study was performed to understand an application of the dental OCT system for measuring the subsurface defect, such as caries.

B-scan was performed up to a depth of 2 mm from the tooth surface. Figure 5 shows part of the image of the corresponding B-scan of the tooth sample. A dental defect was identified in the image at a depth of 105 µm from the surface of the tooth. Further studies are also planned in order to retrieve the spatial extension of the defect by modifying the SLED light beam scanning arrangement.

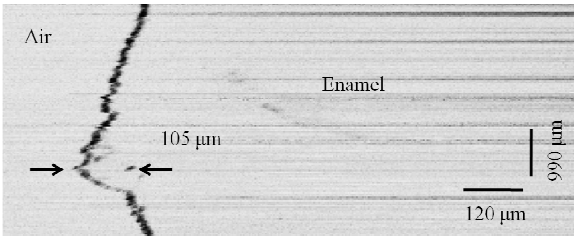

Fig. 5. B-scan image of a carious tooth

A tooth under high demineralisation, lead to cavity formation where there is loss of tooth substance. Such loss of mineral is restored by using composite filling in order to retain the structural integrity of the tooth and to stop the demineralisation from progressing towards the pulp or bone. A tooth sample with a thin composite filling layer was imaged to identify the restoration boundary. A composite resin filling Esthet.X HD (Dentsply) was used to make the filling. Figure 6 shows the B-scan of the filling material. The top surface of the filling and the bonding interface is clearly shown in the Fig. 6. A few bright spots have been identified in the bonding interface and below the filling indicating the presence or void or defects. The streak artifacts in Fig.5 and 6 are due to variation in the background DC component in the interference signal. Based on above studies, fine tuning of the reference arm using electro-optic based scanning technique near the defects can assist in high-resolution imaging of defects/voids.

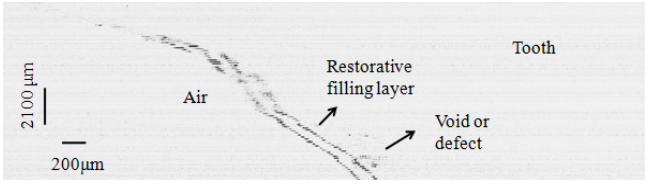

Fig.6. B-scan image of a tooth with composite filling

B. Electro-optic tuning

The electro-optic based scanning technique was studied using Lithium Niobate ($LiNbO_3$) (9×9×25 mm) and Potassium Titanyl Phosphate ($KTiOPO_4$, KTP) (3×3×12) crystals using Helium-Neon laser and Diode laser. The crystal is placed in the reference arm of the OCT setup. In order to compensate the initial path-length difference due to the wavelength dependence of the refractive index a similar crystal was also placed in the sample arm. On applying

electric field only to the crystal in the reference arm, the optical path-length experienced by light passing through the crystal varies - mimicking the mirror movement. The change in optical path-length upon applied voltage is studied by counting the number of fringe shifts. Electro-optic tuning for SLED source was simulated and verified experimentally and the fringe shifting pattern is shown in Fig. 7. The trend followed by the experimental results was found to be qualitatively similar to simulation results. However, due to the background DC term in the interferogram, poor contrast was observed. The optical path-length difference achieved for $LiNbO_3$ (γ_{22} is 7 pm/V) is 0.63 µm for an applied voltage of 6 kV and that for KTP (γ_{33} is 36.3 pm/V) is 1.26 µm for an applied voltage of 4 kV voltage. In order to improve the scanning range, a crystal with a very high electro-optic coefficient value, such as Potassium Tantalate Niobate ($KTa_{1-x}Nb_xO_3$, KTN) can be considered. The optical path-length difference for KTN (4x3.2x1.5 mm) (s_{11} is 2.2×10^{-14} m^2/V^2) for He-Ne laser source and with an applied voltage of 1 kV, is estimated to be ≈441.9 µm and is compared with the experimental data of $LiNbO_3$ and KTP as shown in Fig. 8.

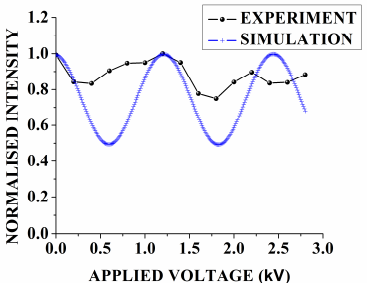

Fig. 7. Electro-optic study with KTP crystal for SLED source

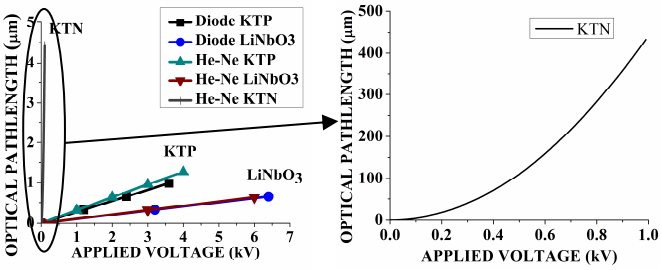

(a) (b)

Fig. 8. (a) Comparative electro-optic study of KTN simulation with $LiNbO_3$ and KTP experimental data and (b) KTN simulation data

V. CONCLUSION

A time domain OCT system was set up in-house for imaging early dental caries and restoration bonding interface. A two-dimensional image of a tooth sample was obtained and a dental defect was identified at a depth of 105 µm from the surface of the tooth. A tooth sample with composite filling was imaged to identify the bonding interfaces. The proposed technique can be used for imaging and measuring the characteristics of the interface between the filler material and the tooth interface. A novel electro-optic tuning system is proposed in order to improve scanning speed and to perform noiseless imaging. Preliminary studies were conducted with $LiNbO_3$ and KTP using He-Ne, Diode laser and SLED sources. In order to increase the range of scanning, a crystal with a higher electro-optic coefficient KTN can be considered. The tuning range is expected to increase to 51.6 µm with an application of a voltage of 1 kV for KTN whereas $LiNbO_3$ and KTP showed a tuning range of 0.63 µm and 1.26 µm for an input voltage of 6 kV and 4 kV, respectively. Thus a significant increase in scanning range can be used for imaging dental caries. However in order to obtain deeper imaging, KTN based hybrid scanning, consisting of an electro-mechanical movement combined with the electro-optic based fine tuning for early dental caries imaging is also planned.

ACKNOWLEDGMENT

Authors are grateful to U. Somasundaram and M.P. Kothiyal for their support and discussions at various stages. Authors are thankful to Dr. Sushila Anand and Dr. R.Suresh, Dental Surgeon, for providing tooth samples. Vani Damodaran is grateful to Department of Science and Technology (DST) for the INSPIRE fellowship to carry out the research work.

REFERENCES

[1] I. A. Pretty, "Caries detection and diagnosis: Novel technologies", *J. Dent.*, vol.34, pp. 727-739, 2006.

[2] Jihoon Na, Jae Ho Baek, Seon Young Ryu, Changsu Lee and Byeong Ha Lee, "Tomographic Imaging of Incipient Dental-Caries Using Optical Coherence Tomography and Comparison with Various Modalities", *Opt Rev*, vol.16, pp.426–431, 2009.

[3] Daniel Fried, John Xie, Sahar Shafi, John D. B. Featherstone, Thomas M. Breunig and Charles Le, "Imaging caries lesions and lesion progression with polarization sensitive optical coherence tomography", *J Biomed Opt*, vol.7, pp.618–627, 2002.

[4] Y. Shimada, A. Sadr, A. Nazari, H. Nakagawa, M. Otsuki, J. Tagami and Y. Sumi, "3D evaluation of composite resin restoration at practical training using swept-source optical coherence tomography (SS-OCT)", *Dent. Mater. J.*, vol.31, pp. 409-417, 2012.

[5] Y. Liang, X. S. Yao, S. Lan, H. Yao, T. Liu, M. Wan, Y. Liang, Y. Li, B. Shi and G. Wang, "Three-Dimensional Image Of The Human Tooth Based On Optical Coherence Tomography", *Progress In Electromagnetics Research C*, vol.8, pp.13–25, 2009.

[6] B. W. Colston, Jr., U. S. Sathyam, L. B. DaSilva, M. J. Everett, P. Stroeve, L. L. Otis, "Dental OCT", *Opt Express*, vol. 3, pp. 230-238, 1998.

[7] W. Drexler and J. G. Fujimoto (*Ed.*), *Optical Coherence Tomography - Technology and Applications,* Springer, New York, pp. 1-40, 2008.

[8] M. Bass, *Handbook of Optics: Fundamentals, techniques, and design*, McGraw-Hill, California, pp. 13.1-13.18, 1995.

[9] J. G. Fujimoto, "Optical Coherence Tomography", *C. R. Acad. Sci.,* vol.2, pp. 1099–1111, 2001.

[10] C. C. Davis, *Lasers and Electro-optics: Fundamentals and Engineering*, Cambridge University Press, Cambridge, pp. 624-635, 1996.

[11] T. A. Maldonado, and T. K. Gaylord, "Electrooptic effect calculations: simplified procedure for arbitrary cases", *Appl. Optics*, vol. 27, pp. 5051-5066, 1988.

[12] N. J. Vasa, Y. Kawata, T. Tanaka and S. Yokoyama, "Development of an electric field sensor based on second harmonic generation with electro-optic materials", *J. Mater. Process. Tech.*, vol. 185, pp. 173-177, 2007.

[13] K. Nakamura, J. Miyazu, Y. Sasaki, T. Imai, M. Sasaura and K. Fujiura, "Space-charge-controlled electro-optic effect: Optical beam deflection by electro-optic effect and space-charge-controlled electrical conduction", *J. Appl. Phys.,* vol. 104, pp. 013105-1 – 013105-10, 2008.